J Appl Biomed
DOI: 10.32725/jab.2022.008
journal homepage: http://jab.zsf.jcu.cz

Journal of Applied Biomedicine

Original research article

Heart rate dynamics in the prediction of coronary artery disease and myocardial infarction using artificial neural network and support vector machine

Rahul Kumar, Yogender Aggarwal *, Vinod Kumar Nigam

Birla Institute of Technology, Department of Bioengineering and Biotechnology, Mesra, Ranchi, Jharkhand, India

Abstract
Background: Atherosclerosis leads to coronary artery disease (CAD) and myocardial infarction (MI), a major cause of morbidity and mortality worldwide. The computer-aided prognosis of atherosclerotic events with the electrocardiogram (ECG) derived heart rate variability (HRV) can be a robust method in the prognosis of atherosclerosis events.
Methods: A total of 70 male subjects aged 55 ± 5 years participated in the study. The lead-II ECG was recorded and sampled at 200 Hz. The tachogram was obtained from the ECG signal and used to extract twenty-five HRV features. The one-way Analysis of variance (ANOVA) test was performed to find the significant differences between the CAD, MI, and control subjects. Features were used in the training and testing of a two-class artificial neural network (ANN) and support vector machine (SVM).
Results: The obtained results revealed depressed HRV under atherosclerosis. Accuracy of 100% was obtained in classifying CAD and MI subjects from the controls using ANN. Accuracy was 99.6% with SVM, and in the classification of CAD from MI subjects using SVM and ANN, 99.3% and 99.0% accuracy was obtained respectively.
Conclusions: Depressed HRV has been suggested to be a marker in the identification of atherosclerotic events. The good accuracy observed in classification between control, CAD, and MI subjects, revealed it to be a non-invasive cost-effective approach in the prognosis of atherosclerotic events.

Keywords: Artificial neural network; Atherosclerosis; Coronary artery disease; Heart rate variability; Myocardial infarction; Support vector machine

Highlights:
- The study revealed reduced heart rate variability (HRV) in CAD and MI patients in comparison to normal subjects.
- The application of a two-class ANN classifier demonstrated 100% classification accuracy in depicting CAD and MI subjects in comparison to control subjects.

Introduction

Cardiovascular diseases (CVDs) cause morbidity and mortality worldwide. The deposition of fatty-streak on the inner wall of arteries causes atherosclerosis-generated CVDs (Shah, 2019). Vascular inflammation has been suggested to be a key mechanism in the progression of atherosclerosis, leading to acute coronary syndromes including myocardial infarction (MI), stroke, and cardiovascular death (Geovanini and Libby, 2018). The autonomic dysfunction was revealed in the pathogenesis of inflammation in atherosclerosis with reduced heart rate variability (HRV) that was inversely correlated with inflammatory markers (Rupprecht et al., 2020). This inflammation increased with the autonomic dysfunction and the decreased vagal mediated inflammatory activity. It has also been demonstrated that the high frequency (HF) band power became lower, reflecting the decreased vagal activity under incremental carotid stenosis. The increased C-reactive protein level has also been suggested to be associated with the decreased vagal activity (Rupprecht et al., 2020).

HRV is defined as the variations in the time series of consecutive RR wave intervals of the electrocardiogram (ECG) waveform. It illustrates the activity of the sympathetic and parasympathetic nervous systems of the autonomic nervous system (ANS) in regulating cardiovascular activity (Shukla and Aggarwal, 2018b). The reduced HRV has been suggested to be correlated with autonomic dysfunction and has been identified as important in the early manifestation of risk factors (Franca et al., 2019; Trivedi et al., 2019). The HRV derived from the R-R interval time series has been suggested to reflect cardiac autonomic activity (Lin et al., 2015; Rupprecht et al.,

* **Corresponding author:** Yogender Aggarwal, Birla Institute of Technology, Department of Bioengineering and Biotechnology, Mesra, Ranchi, Jharkhand, India; e-mail: yaggarwal@bitmesra.ac.in
http://doi.org/10.32725/jab.2022.008
Submitted: 2021-07-20 • Accepted: 2022-06-16 • Prepublished online: 2022-06-21
J Appl Biomed 20/2: 70–79 • EISSN 1214-0287 • ISSN 1214-021X

2020). The hostile behavior that may generate cardiac autonomic imbalance has also been suggested to promote atherosclerosis and cause coronary artery disease (CAD) or mortality (Lin et al., 2015). The higher LF/HF ratio was suggested during neutral and anger. While reduced activation of PNS activity (lower HF) was revealed during recovery in CAD subjects with expressive hostile behavior. Further, suppressive hostility behavior in CAD presented a higher value of LF (SNS and PNS activity) and HF HRV parameters (PNS activation) (Lin et al., 2015). The complex interaction between hemodynamic and humoral is linked with regulators within the autonomic and central nervous system that causes cardiovascular variability (Lanfranchi and Somers, 2002). HRV has also been suggested to have prognostic importance, along with inflammatory markers in predicting CVDs and other diseases (Acharya et al., 2006; Aggarwal et al., 2012; Carney et al., 1988; Laitio et al., 2007; Sajadieh et al., 2006; Shukla and Aggarwal, 2018a, b; Singh et al., 2019; Tarvainen et al., 2014).

The review of the literature suggested application of HRV parameters as input attributes to the support vector machine (SVM), artificial neural network (ANN), probabilistic neural network (PNN), and k-nearest neighbors (KNN) in the classification of coronary artery disease (CAD) with the highest accuracy of 99.2% (Dolatabadi et al., 2017; Lee et al., 2008; Poddar et al., 2019). The HRV features have been utilized in the prediction of hypertension, CAD, and atherosclerosis (Lee et al., 2009; Ni et al., 2018; Verde and De Pietro, 2019). Few studies have suggested the use of wavelet and linear features of heart sound signals as features in the prediction of CAD (Kleiger et al., 1987). Magnetic resonance imaging and Doppler parameters have also been involved in the classification of CVDs (Bento et al., 2019). Further, the work with electrocardiogram (ECG) morphological features has been demonstrated using KNN and convolutional neural network (CNN) with an accuracy of 99.6% (Acharya et al., 2017; Kumar et al., 2017; Sharma and Acharya, 2019; Tan et al., 2018). Coronary artery disease has been suggested to be asymptomatic (Poddar et al., 2019). If untreated, it can lead to the development of ischemia and MI, with heart attack and sudden cardiac death as early symptoms (Poddar et al., 2019). Common diagnostic procedures involve the non-invasive method of electrocardiography and echocardiography. The invasive methods of coronary angiography and cardiac catheterization are costly and time-consuming, requiring a highly specialized person and facility. Although the ECG recording is more commonly available, the invisibility of symptoms of atherosclerotic events on ECG (Dolatabadi et al., 2017) has been suggested to be the major limitation. This can be overcome using the computer-aided technique in the identification of atherosclerosis. The objective of the present study is to extract features of CAD and MI from the recorded ECG waveform using HRV analysis. The obtained features will be utilized to train the machine learning algorithms in predicting the CAD and MI. Thus, the current study has been hypothesized to predict CAD to MI using HRV parameters as features to the SVM and ANN classifiers.

Materials and methods

Participants

A total of 70 male subjects aged 55 ± 5 years participated in the study. Subjects suffering from MI (n = 10) and CAD (n = 30) were selected and recorded. Control subjects (n = 30) were also recorded from the hospital environment that was not diagnosed with any disease. Subjects suffering from CAD and MI with comorbidities that may influence the autonomic functions, including diabetes, autoimmune disease, heart failure, stroke, pulmonary hypertension, lung disease, renal failure, and neurodegenerative disorders have been excluded from the study. Subjects with any medication that directly or indirectly affect the autonomic functions have also been excluded from the study. Meanwhile, adult subjects with clinically confirmed CAD and MI were used in the present study. The subjects were advised to avoid caffeine, nicotine, alcohol, and exercise at least 24 h before the start of the recording procedure. The recording was performed with approval from the Departmental Review Board (BT/RES/2021/01) as per the Declaration of Helsinki guidelines. Signed consent was also received from the subjects before the recording.

ECG recording and pre-processing

The digital lead II ECG was recorded of 10-min duration in the supine position from 10 AM to 12 Noon. The ECG was sampled at 200 samples/s. The SS2LB lead wire was used to connect the MP45 bio amplifier to the disposable electrodes. The Acqknowledge 4.0 software (Biopac Systems Inc., USA) was optimized with gain factor (×1000) and bandpass filter (0.05 to 35 Hz) settings used in acquiring the ECG signal. The linearization of the baseline was obtained by filtering the acquired signal with a 2 Hz high pass filter.

Heart rate variability analysis

The tachogram was obtained from a filtered ECG signal of a five-minute duration using Acqknowledge 4.0 (Biopac Systems Inc., USA). A total of 10 samples were collected from each subject with a shift of 30s duration on recorded ECG signal (Heart rate variability…, 1996). No masking was applied in the calculation of the HRV parameters. The complete recorded ECG signal was used in the calculation of HRV parameters and feature extraction. As per the suggestions of the expert clinician, the data were recorded blindly from the subjects, considering that there was no major comorbidity. The R-waves were located using a QRS detector with a heart rate (30 bpm to 240 bpm). The spline resampling frequency was taken at 8 Hz. The very low frequency (VLF), low frequency (LF), and high frequency (HF) range were set to 0.0–0.04 Hz, 0.04–0.15 Hz, and 0.15–0.40 Hz, respectively. The HRV parameters were obtained from the tachogram using Kubios HRV software V2.0 (University of Eastern Finland, Kuopio, Finland). The physiological interpretations of HRV parameters are illustrated in Table 1.

Time domain parameters

The time-domain analysis involved the mean value of R-R wave interval (mRR), average heart rate (mHR), a standard deviation of R-R interval (SDNN), square root of the mean squared differences of successive R-R interval (rMSSD), triangular index (TI), triangular interpolation of R-R intervals (TiNN), a standard deviation of heart rate (SDHR), count of successive R-R interval >50 ms (NN50), and the ratio of NN50 to the total R-R intervals count (pNN50).

Frequency domain parameters

In the frequency domain, LF, and HF spectral parameters were obtained from the Fourier transformation method. Further, the autonomic balance as predicted from the ratio of LF to HF was also calculated. On the contrary, studies have suggested that the LF and LF/HF ratio reflects the baroreflex function and not the sympathetic tone (Goldstein et al., 2011; Rahman et al., 2011).

Table 1. Physiological Interpretation of heart rate variability parameters

HRV parameters	Units	Description	SNS/PNS activity	References
mRR	ms	Mean of R-R interval of ECG waveform	PNS	Acharya et al., 2006
SDNN	ms	Standard deviation of R-R interval	PNS	Guan et al., 2018
mHR	bpm	Mean heart rate	SNS	Aggarwal et al., 2018b
SDHR	bpm	Heart rate standard deviation	SNS	Aggarwal et al., 2018b
rMSSD	ms	The square root of the average squared differences between adjacent RR intervals	PNS	Guan et al., 2018
NN50	count	Count of R-R intervals differing >50 ms	PNS	Guan et al., 2018
pNN50	% count	Percentage of R-R interval that differs >50 ms	PNS	Guan et al., 2018
Ti	a.u.	Total number of NN intervals divided by the height of histogram	PNS	
TiNN	ms	Triangular interpolation of the highest peak of the histogram	PNS	
LF	n.u.	Low frequency component	Baroreflex activity	Goldstein et al., 2011; Rahman et al., 2011).
HF	n.u.	High frequency component	PNS	Guan et al., 2018
LF/HF	a.u.	Ratio of LF to HF normalized powers	Baroreflex activity	Goldstein et al., 2011; Rahman et al., 2011).
SD1	ms	Standard deviation of peak to peak interval perpendicular to the line of identity	PNS	Shaffer and Ginsberg, 2017
SD2	ms	Standard deviation of peak to peak interval along the line of identity	SNS and PNS	Orellana et al., 2015
SD2/SD1	a.u.	Ratio of SD2 to SD1	SNS	Behbahani et al., 2012
Lmean	beats	Mean length of the diagonal lines in the recurrence plot	SNS and PNS	Takakura et al., 2017
Lmax	beats	The longest diagonal line in the recurrence plot	PNS	Takakura et al., 2017
REC	%	The ratio of ones and zeros in the recurring plot matrix	SNS and PNS	Takakura et al., 2017
DET	%	Determinism represents the percentage of REC points that form diagonal lines		
ShanEn	a.u.	Shannon Entropy of diagonal length distribution	PNS	Schlenker et al., 2014
ApEn and SampEn	a.u.	Approximate and Sample entropy parameters determine the irregularity in the signal	PNS	Schlenker et al., 2014
Alpha 1 and Alpha 2	a.u.	Alpha 1 and Alpha 2 represents low scale and high scale detrended fluctuation slope	PNS	Shukla and Aggarwal, 2018a
CD	a.u.	The correlation dimension revealed the signal complexity	PNS	Shukla and Aggarwal, 2018a

ms – mili second; bpm, beats per minute; a.u. – arbitrary unit; n.u. – normalized unit; SNS – sympathetic nervous system; PNS – parasympathetic nervous system, respectively.

Nonlinear domain parameters

The nonlinear methods measure the complexity of RRi. The different parameters include the Poincare plot (PP) with short (SD1) and long-term variability (SD2), with RRi points above or below the line of identity on the elliptical-shaped plot. The entropy approximate (ApEn) and sample entropy (SampEn) reflects the signal complexity, and are used in measuring the randomness of heart rhythm. The short (α1) and long (α2) detrended fluctuation analysis (DFA) removes the linear trends in the nonlinear signal. The correlation dimension (CD) value measured the line patterns (saturated at finite value) with varying heart rates (HR). The recurrence plot signifies the time, the line is parallel to the main diagonal line (Tarvainen et al., 2014).

Features and classification algorithm

All the HRV parameters in different domains were selected to train and test the classification accuracy using ANN and SVM. The time, frequency, and nonlinear domain parameters were grouped and used as input nodes to the ANN model. The two-class networks were optimized for best accuracy in the classification of MI and CAD from control subjects. 80% of the dataset was used for the training and 20% for the testing of both models. The performance metrics were also evaluated from the obtained confusion matrix as mentioned below (Baratloo et al., 2015):

- Sensitivity = [TP/(TP + FN)]*100
- Specificity = [TN/(TN + FP)]*100
- Accuracy = f(TP + TN)/(TP + TN + FP + FN)]*100
- Precision = [TP/(TP = FP)]*100

TP, true positive; TN, true negative; FP, false positive; FN, false negative

Backpropagation ANN model for classification of MI and CAD

Python language (Anaconda, Inc., USA) was used in developing the three-layered backpropagation ANN model. The model consists of 25 nodes in the input layer (IL) and one node in the output layer (OL). The hidden layer (HL) was optimized with varying learning rates (LR). The model was implemented in the prediction of CAD and MI subjects from the controls. The value of twenty-five HRV features was used to train the

ANN model. The activation function (ReLU), y = max (0, x) was used at hidden layer nodes. The LR range from 0.001 to 0.1 was assigned to the model for optimization of HL nodes at 10000 epochs. The sigmoid activation function ($f(z) = 1 / 1 + e^{-z}$) was used at the output node to predict the target.

Support vector machine

The SVM distinguishes the two hyperplane data points with distance minimization. The optimized hyperplane was estimated by the SVM, with box constraint (C) > 0. The radial basis function kernel was used with scale (γ) > 0 for optimized SVM. The algorithm was programmed in Python using the Anaconda programming language. The twenty-five HRV features were used as input to SVM. The kernel was optimized with C and γ values ranging from 0.001 to 10 and 0.001 to 1, respectively.

Statistical analysis

One-way ANOVA was performed to test significant differences between the independent samples of different sizes originating from the Control, CAD, and MI subjects. The quantitative data on time, frequency, and nonlinear domain of the HRV analysis was used for the statistical analysis. The null hypothesis selected was 'At least one group mean is different from other groups'. The code was written and designed in Python V3.6.8 to analyze the test at $P < 0.05$. The study procedure in deriving the HRV parameters from the ECG signal and the application of machine learning algorithms is shown in Fig. 1.

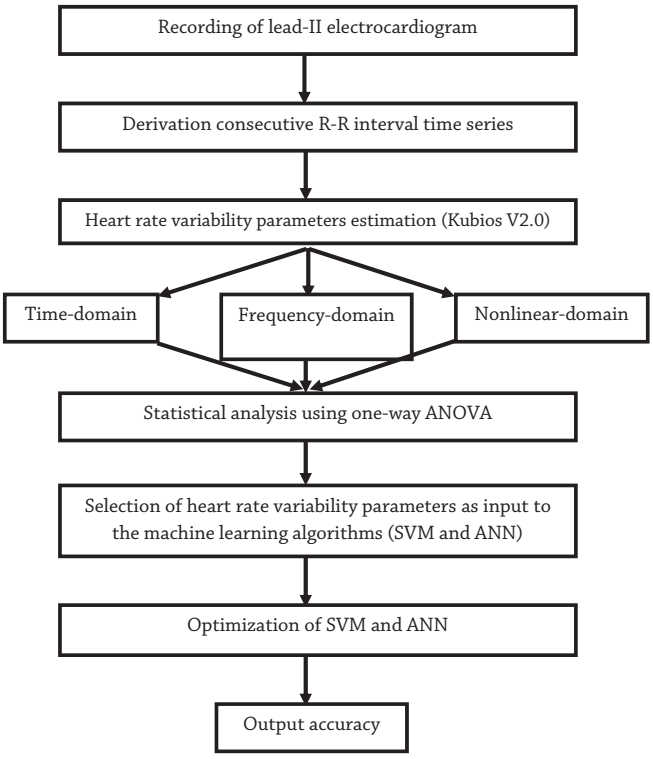

Fig. 1. Flowchart depicting the study procedure

Results

In the present study, the HRV features were extracted from the ECG signal of CAD (n = 30) and MI (n = 10) subjects. Statistically, the one-way ANOVA test demonstrated significant difference exits between the CAD, MI, and Control (n = 30) groups. A flowchart summarising the subjects' flow through the study is illustrated in Fig. 2.

Heart rate variability analysis in atherosclerosis

The obtained HRV results revealed a significantly lower value of mRR (F = 3.80, P = 0.02) in both CAD and MI in comparison to the control subjects. Further the value was observed to be lower in MI group than in the CAD group (Fig. 3). mHR (F = 17.70, $P < 0.0001$) value was found to be significantly higher in both the CAD and MI groups than in the control subjects. Further, the MI group exhibited higher mHR values than in the CAD subjects ($P < 0.0001$) (Fig. 4). Further, the value of LF (F = 2.83, P = 0.05) and SD2 (F = 7.64, P = 0.0005) parameters were also observed to be significantly lower in the CAD subject than in the Control group. While the value of LF (P = 0.1875) and SD2 (P = 0.1463) was found to be lower in MI subjects in comparison to the control group. However, the value was not found to be statistically significant. Further, the value of LF (P = 0.0030) and SD2 (P = 0.0173) parameters were found to be significantly higher in MI subjects than in the CAD subjects (Fig. 4).

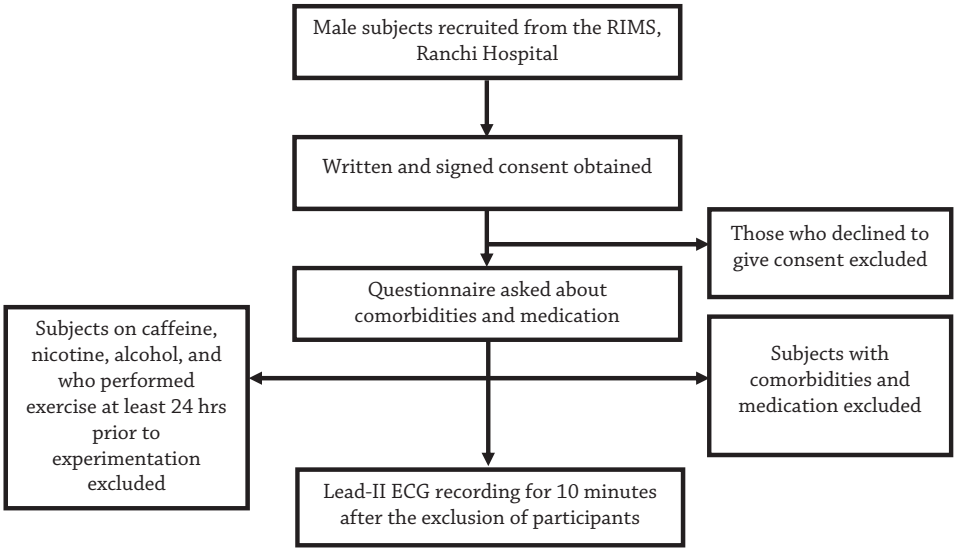

Fig. 2. A flowchart summarizing participant flow through the study

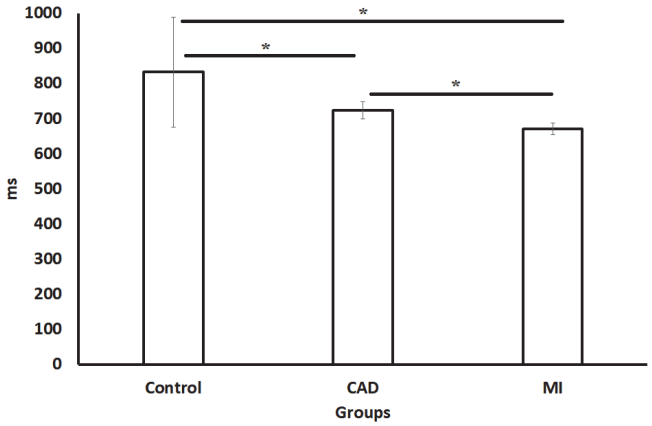

Fig. 3. The change in mRR (mean R to R interval) (mean ± SD, $P < 0.05$) in-effect to Control, CAD and MI subjects. CAD and MI represent coronary artery disease and myocardial infarction, ms – millisecond and SD – standard deviation. Asterisk * indicates a statistically significant difference.

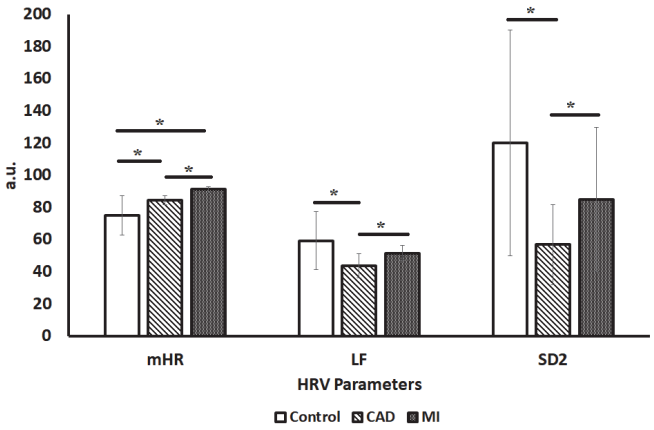

Fig. 4. The chart demonstrates variations in mHR, SD2 and LF parameters in Control, CAD and MI subjects (mean ± SD, $P < 0.05$). CAD and MI represent coronary artery disease and myocardial infarction, SNS – sympathetic nervous activity, a.u. – arbitrary unit, mHR – mean heart rate, LF – low frequency, SD2 – standard deviation of peak to peak interval along the line of identity and SD – standard deviation. Asterisk * indicates a statistically significant difference.

The value of the SD1 ($F = 3.01$, $P = 0.04$) parameter was found to be lower in CAD ($P = 0.0031$) and MI ($P = 0.0076$) subjects than in the control subjects. However, there was a trend for SD1 to be lower in MI than in the CAD subjects however did not reach the statistical significance ($P = 0.1520$). The value of SDNN ($P = 0.0001$) and rMSSD ($P = 0.0025$) were significantly lower in CAD group than in the control group (Fig. 5). Although, the value of SDNN ($P = 0.0694$) and rMSSD ($P = 0.3192$) were also observed to be lower in MI group in comparison to the control subjects but failed to define the statistical significance. MI subjects also exhibited a higher value than the CAD subjects in both SDNN ($P = 0.3511$) and rMSSD ($P = 0.2081$) parameters but did not reach statistical significance (Fig. 5). The value of the Lmax parameter was found to be significantly lower in CAD ($P < 0.0001$) and MI ($P < 0.0001$) subjects than in the control subjects. Further, the trend was observed for Lmax to be lower in MI than in the CAD subjects and found to be statistically significant ($P = 0.0160$) (Fig. 5). A higher value of the TiNN parameter was observed in both the CAD ($P = 0.2380$) and MI ($P = 0.9993$) subjects in comparison to the control group however the value was found to be insignificant. While the value was found to be lower in MI than in the CAD subjects but failed to reach the significance ($P = 0.4000$) (Fig. 5).

The value of Ti, NN50 and pNN50 HRV parameters were found to be significant lower in both the CAD ($P < 0.0001$, $P < 0.0001$ and $P < 0.0001$ respectively) and MI ($P < 0.0001$, $P < 0.0001$ and $P = 0.0164$ respectively) group than in the control subjects. Further, a higher value of Ti, NN50 and pNN50 in MI ($P < 0.0001$, $P < 0.0001$ and $P = 0.0002$ respectively)

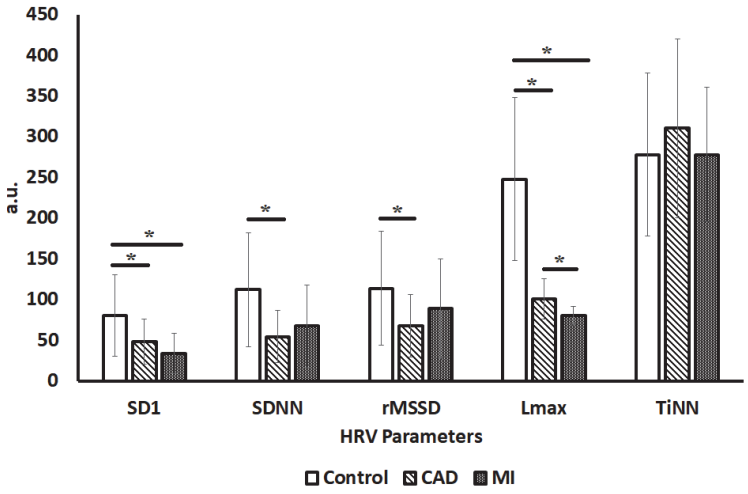

Fig. 5. The HRV parameters SD1, SDNN, rMSSD, Lmax and TiNN reflect the change in PNS activity under Control, CAD and MI subjects (mean ± SD, $P < 0.05$). CAD and MI represent coronary artery disease and myocardial infarction, HRV – heart rate variability, a.u. – arbitrary unit, PNS – parasympathetic nervous system, SD1 – standard deviation of peak to peak interval perpendicular to the line of identity, SDNN – standard deviation of R-R interval, rMSSD – square root of the average squared differences between adjacent RR intervals, Lmax – longest diagonal line in the recurrence plot, TiNN – triangular interpolation of the highest peak of the histogram and SD – standard deviation. Asterisk * indicates a statistically significant difference.

subjects than in the CAD group and define the statistically significant difference. Although a significantly higher value of HF was observed in the CAD (P < 0.0001) and MI (P = 0.0430) group in comparison to the control group. Further, MI subjects exhibited lower values than the CAD subjects but failed to define the statistical significance (P = 0.1164). The Lmean value also found to be in CAD (P = 0.0646) and MI (P = 0.2571) groups however did not reach the statistical significance (Fig. 6).

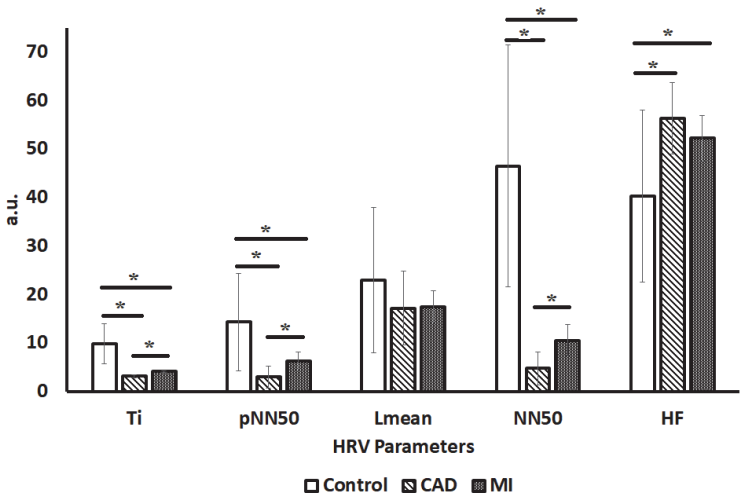

Fig. 6. The HRV parameters, Ti, pNN50, Lmean, NN50 and HF (mean ± SD, P < 0.05) reflect the change in parasympathetic activity in Control, CAD and MI Subjects. where CAD and MI represent coronary artery disease and myocardial infarction, HRV – heart rate variability, a.u. – arbitrary unit, Ti – total number of NN intervals divided by the height of histogram, pNN50 – percentage of R-R interval that differs >50 ms, Lmean – mean length of the diagonal lines in the recurrence plot, NN50 – count of R-R intervals differing >50 ms, HF – high frequency and SD – standard deviation. Asterisk * indicates a statistically significant difference.

The approximate entropy analysis revealed significantly lower values in CAD (P <0.0001) and MI (P < 0.0001) as compared to control subjects. MI subjects demonstrated marginal lower values in comparison to CAD subjects however failed to define the statistical significance (P = 0.9985) (Fig. 7).

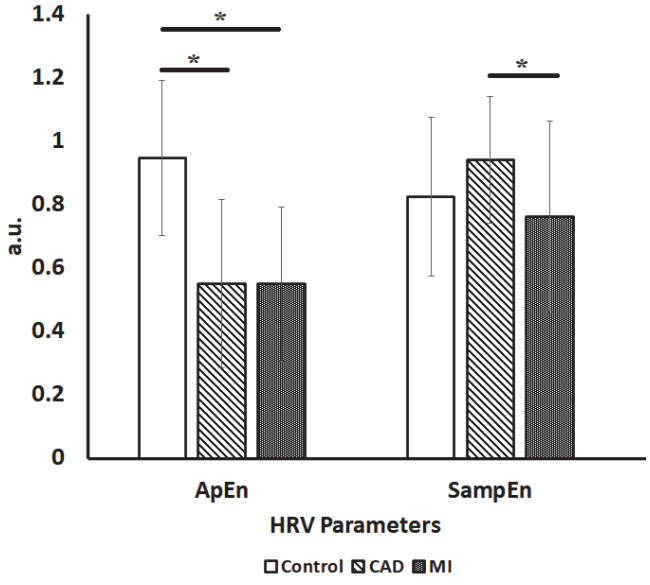

Fig. 7. The chart demonstrates the variation in approximate (ApEn) and sample (SampEn) entropy parameters in Control, CAD and MI subjects (mean ± SD, P < 0.05). CAD and MI represent coronary artery disease and myocardial infarction, a.u. – arbitrary unit and SD – standard deviation. Asterisk * indicates a statistically significant difference.

The Sample entropy analysis demonstrated an insignificant higher value in CAD (P = 0.0512) and a lower value in MI (P = 0.5147) subjects as compared to the control subjects. Further, the statistically significant value was found to be lower in MI subjects than the CAD subjects (P = 0.0373) as shown in Fig. 7. The α1 (F = 14.38, P = 0.0001), α2 (F = 30.01, P < 0.0001) and CD (F = 60.53, P = 0.0001) results revealed significantly lower values in CAD (P < 0.0001, P < 0.0001 and P < 0.0001 respectively) and MI (P = 0.0070, P < 0.0001 and P <0.0001 respectively) compared to the control group. The marginal

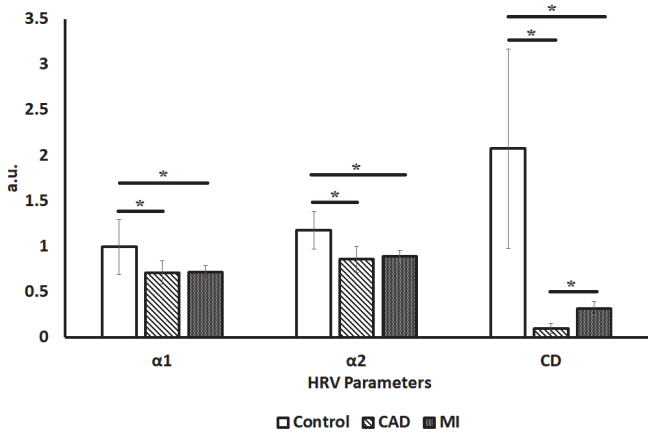

Fig. 8. The detrended fluctuation analysis (α1 and α2) and correlation dimension (CD) in differentiating the control, CAD, and MI subjects (mean ± SD, P < 0.05). CAD and MI represent coronary artery disease and myocardial infarction, a.u. – arbitrary unit and SD – standard deviation. Asterisk * indicates a statistically significant difference.

lower α1 and α2 values were observed in CAD (P = 0.8860 and P = 0.5679 respectively) than MI subjects however the difference was found to be statistically not significant. A significant difference was found in CD values of CAD and MI subjects (P < 0.0001) (Fig. 8). The SDHR, LF/HF and ShanEn were found to have significantly lower in the CAD (P = 0.0204, P = 0.0004 and P = 0.0003 respectively) group as compared to the control groups. Higher value of SDHR (p = 0.2799) was found to be insignificant between control and MI. Further, increased value of MI was observed in MI as compared to CAD. However, the difference did not reach the statistically significant (p = 0.322) (Fig. 9). The value of LF/HF, SD2/SD1 and ShanEn were observed to be significantly lower in MI subjects than in the control group (P = 0.0465, p = 0.0364 and P = 0.0158 respectively). The REC (P = 0.0077) and DET (P = 0.0083) parameters demonstrated a significant difference with lower values in MI as compared to the CAD subjects as shown in Fig. 9.

Two-class machine learning in the prediction of CAD and MI events

The ANN architecture was optimized first the varying LR from 0.001 to 0.9 with fixed hidden nodes number to 13. The optimized LR was selected with the highest classification accuracy. Secondly, the number of hidden nodes varied from 13 to 65 in the hidden layer and kept the LR at an optimized rate. The optimized ANN architecture and SVM were used to classify CAD and MI events, as presented in Table 2.

The obtained results demonstrated 100% accuracy in the classification of CAD and MI subjects from the control subjects using ANN. SVM had an accuracy of 99.6%. An accuracy of 99.3% and 99.0% was obtained in the classification of CAD from MI subjects using SVM and ANN, respectively (Table 2). The performance metrics in evaluating the SVM and ANN model for the obtained training accuracy are illustrated in Table 3.

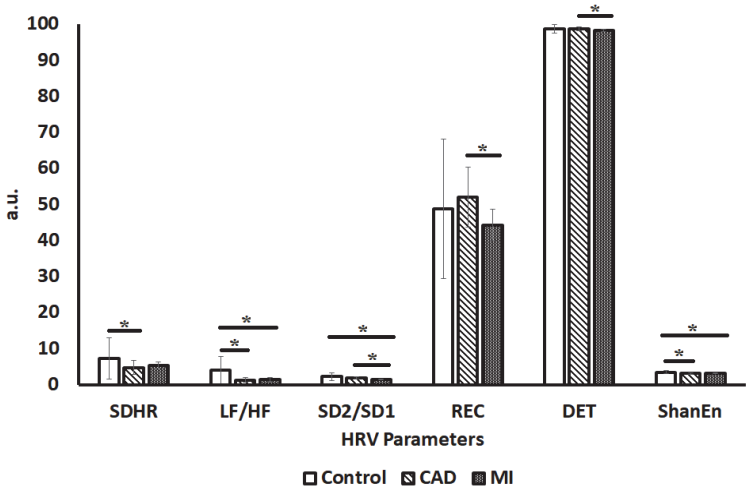

Fig. 9. Heart rate variability parameters SDHR, LF/HF, SD2/SD1, REC, DET and ShanEn in the comparison of control, CAD, and MI subjects (mean ± SD, P < 0.05). CAD and MI represent coronary artery disease and myocardial infarction, a.u. – arbitrary unit, SDHR – standard deviation of Heart rate, LF/HF – ratio of LF to HF, SD2/SD1 – ratio of SD2 to SD1, REC – the ratio of ones and zeros in the recurring plot matrix, DET – determinism represents the percentage of REC points that form diagonal lines, ShanEn – Shannon Entropy of diagonal length distribution and SD – standard deviation. Asterisk * indicates a statistically significant difference.

Table 2. Artificial neural network (ANN) and support vector machine (SVM) two-class architecture in the classification of atherosclerotic events

Case	Class I	Class II	SVM (%)	Optimized SVM model	ANN (%)	Optimized ANN architecture (LR)
1	CAD	MI	99.3	(C = 3, γ = 0.07)	99.0	25:26:1 (0.1)
2	Control	CAD	99.6	(C = 3, γ = 0.001)	100	25:13:1 (0.1)
3	Control	MI	99.6	(C = 8, γ = 0.04)	100	25:13:1 (0.01)

CAD and MI for coronary artery disease and myocardial infarction, respectively. LR for learning rate, C box constraint, and γ radial basis function kernel scale.

Table 3. Performance metrics of the machine learning model used in the classification of CAD and MI subjects from the control group

			Performance metrics (%)			
Class 1	Class 2	Model	Sensitivity	Specificity	Accuracy	Precision
Control	CAD	SVM	99.2	100	99.6	100
Control	MI	SVM	99.6	100	99.6	100
CAD	MI	SVM	99.2	100	99.3	100
Control	CAD	ANN	100	100	100	100
Control	MI	ANN	100	100	100	100
CAD	MI	ANN	98.8	100	99.0	100

CAD, MI, SVM and ANN for coronary artery disease, myocardial infarction, support vector machine, and artificial neural network, respectively.

Discussion

This study was undertaken to predict CAD and MI events of atherosclerosis using HRV parameters. The obtained results demonstrated withdrawal of PNS tone with higher SNS activity to maintain the autonomic balance, causing depressed HRV in CAD and MI subjects in comparison to control subjects. Two-class classifiers were implemented in the classification of atherosclerotic events. An accuracy of 100% was obtained in classifying the CAD and MI subjects from controls using ANN. An accuracy of 99.3% was obtained in the classification of CAD and MI subjects using SVM. The applications of HRV parameters in the prognosis of the diseases are limited at the research level but not in clinical practice. This may be due to varied agreement on the efficacy and accuracy of HRV in the clinical diagnosis. Further, the autonomic function may vary with other comorbidities. Thus, future work will be enhanced by the inclusion of more samples of varied gender, age groups, and other comorbidities in analyzing the HRV parameters, with a larger test dataset in training and testing the machine learning model proposed in the present study. The outcome of future work will help to design and develop a robust computer-assisted approach for clinical use.

Heart rate variability analysis in autonomic function

A review of the literature revealed SNS dominance with PNS withdrawal to maintain autonomic balance under low HRV. While higher HRV value demonstrated a shift of autonomic balance towards increased vagal tone (Xhyheri et al., 2012). The observed results were in line with previous findings that suggested PNS impairment with the dominance of LF and lowered time domain parameter in CAD (Abdelnabi, 2019; Carney et al., 2001; Xhyheri et al., 2012). Further, the lower value of SDNN was demonstrated to be an independent factor in predicting mortality in post-surgery MI patients (Kleiger et al., 1987).

It has been revealed that the higher risk of mortality and morbidity with decreased HRV in CAD depressed patients reflects autonomic dysregulation (Tristani et al., 1977). The reduced HRV was also suggested to be associated with rapid subintimal lipid accumulation, leading to coronary narrowing (Huikuri et al., 1999). The SDNN was observed to predict intima-media thickness and progression of coronary atherosclerosis. Further, the atherosclerotic process was also revealed to be correlated with autonomic dysregulation in the frequency domain (Manfrini et al., 2008). Lower vagal tone was suggested to cause coronary vasoconstriction through loss of PNS mediated vasodilation (Xhyheri et al., 2012). This withdrawal of PNS was suggested to cause coronary instability resulting in coronary ischemia with worsened prognosis (Heusch, 2011).

Further, Singer and co-workers demonstrated a prediction of mortality among patients undergoing coronary angiography with low HRV (Maheshwari et al., 2016). A significant increase in LF and decrease in HF corresponding to sympathetic activation and reduced vagal tone were also suggested, and SNS plays a major role in the progression of heart failure (Sztajzel, 2004). The decreased SDNN HRV measures in MI patients and after MI has suggested a higher risk of mortality (Buccelletti et al., 2009; Stein and Kleiger, 1999). The mean HR was reported to be higher in CAD patients, revealing the role of increased sympathetic activity. This also promotes the manifestation of ischemic heart diseases, lethal arrhythmias, or increased atherosclerosis (Carney et al., 1988). The value of LF/HF was demonstrated to be lower in patients with MI (Quintana et al., 1997). Recently, the increase and decrease in LF and HF respectively were also suggested two weeks after MI. While the reverse was observed at six to twelve months after MI (Abdelnabi, 2019). Further, a lower value of SDNN was reported in acute MI subjects and associated with increased mortality (Abdelnabi, 2019; Kleiger et al., 1987). The CAD patients have been suggested to have a lower value of NN50 and pNN50 in comparison to normal subjects (Acharya et al., 2014). While higher value was observed in SampEn and ApEn (Shi et al., 2019).

Analysis of machine learning approaches

The SVM and ANN presented an accuracy of 99.6% and 100% in depicting the CAD and MI subjects from controls, respectively using SVM and ANN. The published findings revealed an accuracy of 99.2%, 90%, and 80% in the classification of CAD using SVM, PNN, and KNN (Dolatabadi et al., 2017; Poddar et al., 2019). In another study, accuracy of 85% and 70% were also reported in depicting CAD with the SVM technique (Lee et al., 2008). Further, an accuracy of 99.1% was demonstrated with ANN and K-fold validation in the detection of MI subjects (Shahnawaz and Dawood, 2021). Sopic et al. (2018) attained an accuracy of 83.26% in the classification of MI using time and frequency domain features with a random forest classifier.

Singh et al. (2022) demonstrated an accuracy of 99.76% and 100% in the prediction of young and elderly CAD subjects using HRV features with generalized discriminant analysis.

Shi et al. (2019) suggested Renyi Distribution Entropy features in the prediction of CAD with an accuracy of 97.5% with KNN. The wavelet and linear features of the heart sound signal revealed an accuracy of 85% and 90% using ANN and SVM, respectively (Karimi et al., 2005; Kleiger et al. 1987). ECG morphological features-based work had an accuracy of 79.2% to 99.6% using SVM, KNN, and CNN as a classifier (Acharya et al., 2017; Kumar et al., 2017; Sharma and Acharya, 2019; Tan et al., 2018). The imaging feature extracted from magnetic resonance and doppler technique demonstrated an accuracy of 97.5% and 81.4% using SVM (Bento et al., 2019). The ANN and SVM models were demonstrated to classify the diabetic and control subjects with an accuracy of 96.2% and 95.2% using time-domain HRV features (Aggarwal et al., 2021). While, in another study, the nonlinear HRV parameters were used to classify the diabetic subjects with an accuracy of 86.3% and 90.5% using ANN and SVM, respectively (Aggarwal et al., 2020). Time-domain parameters of HRV have been used for the classification of diabetes from control subjects (rat model) using ANN and SVM model, and 96.2% and 65.2% accuracy has been achieved (Agarwal et al., 2021). Further, non-linear domain parameters of HRV have also been used for the classification of diabetes from control subjects (rat model) using the ANN and SVM model, and 86.3% and 90.5% accuracy have been achieved (Agarwal et al., 2020).

Limitations and future direction

The major limitation of the present work is the low sample size. Also, other comorbidities have not been considered. The single-channel digital ECG was recorded for only 10 minutes to extract the HRV features. The applications of HRV analysis in the diagnosis of autonomic function are limited at the research level and not in clinical practice. This may be due to varied agreement on the efficacy and accuracy of HRV in the clinical diagnosis. Further, the assessment of HRV with other comorbidities needs to be studied, which may impact the HRV analysis. The work will be enhanced with the inclusion of more samples of varied gender and age groups in analyzing the HRV

parameters and creating a larger test dataset in testing the ANN and SVM model proposed in the present study. The outcome of future work will help to design and develop a robust computer-assisted approach for clinical use.

Conclusions

The investigation demonstrated depressed HRV in CAD and MI patients in comparison to normal subjects. The proposed system, utilizing twenty-five HRV features, presented an accuracy of 100% in predicting CAD and MI subjects from control subjects. Thus, this non-invasive and cost-effective computer-assisted method can be automatically implemented in the early prediction of CAD and MI conditions.

Ethical aspects and conflict of interests

The authors have no conflict of interests to declare.

Acknowledgements

The authors are grateful to Dr. Prabin Kumar Shrivastava of Rajendra Institute of Medical Sciences, Ranchi, for collecting electrocardiogram data. The authors are also thankful to Mr. Rohit Kumar of Birla Institute of Technology, Ranchi, for his support in implementing the machine learning technique. Authors are also grateful to CSIR-UGC for senior research fellowship to Mr. Rahul Kumar, Birla Institute of Technology, Ranchi.

References

Abdelnabi MH (2019). Cardiovascular clinical implications of heart rate variability. Int J Cardiovasc Acad 5: 37–41. DOI: 10.4103/IJCA.IJCA_36_18.

Acharya UR, Faust O, Sree V, Swapna G, Martis RJ, Kadri NA, et al. (2014). Linear and nonlinear analysis of normal and CAD-affected heart rate signals. Comput Methods Programs Biomed 113: 55–68. DOI: 10.1016/j.cmpb.2013.08.017.

Acharya UR, Joseph KP, Kannathal N, Lim CM, Suri, JS (2006). Heart rate variability: a review. Med Biol Eng Comput 44: 1031–1051. DOI: 10.1007/s11517-006-0119-0.

Acharya UR, Sudarshan VK, Koh JE, Martis RJ, Tan JH, Oh SL (2017). Application of higher-order spectra for the characterization of coronary artery disease using electrocardiogram signals. Biomed Signal Process Control 31: 31–43. DOI: 10.1016/j.bspc.2016.07.003.

Aggarwal Y, Das J, Mazumder PM, Kumar R, Sinha RK (2020). Heart rate variability features from nonlinear cardiac dynamics in identification of diabetes using artificial neural network and support vector machine. Biocybern Biomed Eng 40: 1002–1009. DOI: 10.1016/j.bbe.2020.05.001.

Aggarwal Y, Das J, Mazumder PM, Kumar R, Sinha RK (2021). Heart rate variability time domain features in automated prediction of diabetes in rat. Phys Eng Sci Med 44: 45–52. DOI: 10.1007/s13246-020-00950-8.

Aggarwal Y, Singh N, Sinha RK (2012). Electrooculogram based study to assess the effects of prolonged eye fixation on autonomic responses and its possible implication in man-machine interface. Health Technol 2: 89–94. DOI: 10.1007/s12553-011-0012-1.

Baratloo A, Hosseini M, Negida A, El Ashal G (2015). Part 1: Simple definition and calculation of accuracy, sensitivity and specificity. Emerg (Tehran) 3: 48–49.

Behbahani S, Dabanloo NJ, Nasrabadi AM (2012). Ictal heart rate variability assessment with focus on secondary generalized and complex partial epileptic seizures. Adv Biores 4: 50–58.

Bento M, Souza R, Salluzzi M, Rittner L, Zhang Y, Frayne R (2019). Automatic identification of atherosclerosis subjects in a heterogeneous MR brain imaging data set. Magn Reason Imaging 62: 18–27. DOI: 10.1016/j.mri.2019.06.007.

Buccelletti E, Gilardi EM, Scaini E, Galiuto LE, Persiani RO, Biondi AL, et al. (2009). Heart rate variability and myocardial infarction: systematic literature review and metanalysis. Eur Rev Med Pharmacol Sci 13: 299–307.

Carney RM, Blumenthal JA, Stein PK, Watkins L, Catellier D, Berkman LF, et al. (2001). Depression, heart rate variability, and acute myocardial infarction. Circulation 104: 2024–2028. DOI: 10.1161/hc4201.097834.

Carney RM, Rich MW, TeVelde A, Saini J, Clark K, Freedland KE (1988). The relationship between heart rate, heart rate variability and depression in patients with coronary artery disease. J Psychosom Res 32: 159–164. DOI: 10.1016/0022-3999(88)90050.

Dolatabadi AD, Khadem SE, Asl BM (2017). Automated diagnosis of coronary artery disease (CAD) patients using optimized SVM. Comput Methods Programs Biomed 138: 117–126. DOI: 10.1016/j.cmpb.2016.10.011.

Franca da Silva AK, Destro Christofaro DG, Manata Vanzella L, Marques Vanderlei F, Lopez Laurino MJ, Vanderlei M (2019). Relationship of the aggregation of cardiovascular risk factors in the parasympathetic modulation of young people with type 1 diabetes. Medicina (Kaunas) 55: 534. DOI: 10.3390/medicina55090534.

Geovanini GR, Libby P (2018). Atherosclerosis and inflammation: overview and updates. Clin Sci (Lond) 132: 1243–1252. DOI: 10.1042/CS20180306.

Goldstein DS, Bentho O, Park MY, Sharabi Y (2011). Low-frequency power of heart rate variability is not a measure of cardiac sympathetic tone but may be a measure of modulation of cardiac autonomic outflows by baroreflexes. Exp Physiol 96: 1255–1261. DOI: 10.1113/expphysiol.2010.056259.

Guan L, Collet J-P, Mazowita G, Claydon VE (2018). Autonomic nervous system and stress to predict secondary ischemic events after transient ischemic attack or minor stroke: possible implications of heart rate variability. Front Neurol 9: 90. DOI: 10.3389/fneur.2018.00090.

Heart rate variability: standards of measurement, physiological interpretation and clinical use (1996). Task Force of the European Society of Cardiology and the North American Society of Pacing and Electrophysiology. Circulation 93: 1043–1065.

Heusch G (2011). The paradox of α-adrenergic coronary vasoconstriction revisited. J Mol Cell Cardiol 51: 16–23. DOI: 10.1016/j.yjmcc.2011.03.007.

Huikuri HV, Jokinen V, Syvänne M, Nieminen MS, Airaksinen KJ, Ikäheimo MJ, et al. (1999). Heart rate variability and progression of coronary atherosclerosis. Arterioscler Thromb Vasc Biol 19: 1979–1985. DOI: 10.1161/01.ATV.19.8.1979.

Karimi M, Amirfattahi R, Sadri S, Marvasti SA (2005). Noninvasive detection and classification of coronary artery occlusions using wavelet analysis of heart sounds with neural networks. The 3rd IEE International Seminar on Medical Applications of Signal Processing. 2005: 117–120. DOI: 10.1049/ic:20050342.

Kleiger RE, Miller JP, BiggerJT, Jr., Moss AJ (1987). Decreased heart rate variability and its association with increased mortality after acute myocardial infarction. Am J Cardiol 59: 256–262. DOI: 10.1016/0002-9149(87)90795-8.

Kumar M, Pachori RB, Acharya UR (2017). Characterization of coronary artery disease using flexible analytic wavelet transform applied on ECG signals. Biomed Signal Process Control 31: 301–308. DOI: 10.1016/j.bspc.2016.08.018.

Laitio T, Jalonen J, Kuusela T, Scheinin H (2007). The role of heart rate variability in risk stratification for adverse postoperative cardiac events. Anesth Analg 105: 1548–1560. DOI: 10.1213/01.ane.0000287654.49358.3a.

Lanfranchi PA, Somers VK (2002). Arterial baroreflex function and cardiovascular variability: interactions and implications. Am J Physiol Regul Integr Comp Physiol 283: R815–R826. DOI: 10.1152/ajpregu.00051.2002.

Lee HG, Kim WS, Noh KY, Shin JH, Yun U, Ryu KH (2009). Coronary artery disease prediction method using linear and nonlinear feature of heart rate variability in three recumbent postures.

Inform Syst Front 11: 419–431. DOI: 10.1007/s10796-009-9155-2.

Lee HG, Noh KY, Ryu KH (2008). A data mining approach for coronary heart disease prediction using HRV features and carotid arterial wall thickness. International Conference on Biomedical Engineering and Informatics 1: 200–206. DOI: 10.1109/BMEI.2008.189.

Lin IM, Weng CY, Lin TK, Lin CL (2015). The relationship between expressive/suppressive hostility behavior and cardiac autonomic activations in patients with coronary artery disease. Acta Cardiol Sin 31: 308–316. DOI: 10.6515%2FACS20141027.

Maheshwari A, Norby FL, Soliman EZ, Adabag S, Whitsel EA, Alonso A, Chen LY (2016). Low Heart Rate Variability in a 2-Minute Electrocardiogram Recording Is Associated with an Increased Risk of Sudden Cardiac Death in the General Population: The Atherosclerosis Risk in Communities Study. Plos One 11: e0161648. DOI: 10.1371/journal.pone.0161648.

Manfrini O, Pizzi C, Viecca M, Bugiardini R (2008). Abnormalities of cardiac autonomic nervous activity correlate with expansive coronary artery remodelling. Atherosclerosis 197: 83–189. DOI: 10.1016/j.atherosclerosis.2007.03.013.

Ni H, Cho S, Mankoff J, Yang J (2018). Automated recognition of hypertension through overnight continuous HRV monitoring. J Ambient Intell Humaniz Comput 9: 2011–2023. DOI: 10.1007/s12652-017-0471-y.

Orellana JN, de la Cruz Torres B, Cachadiña ES, de Hoyo M, Dominguez Cobo S (2015). Two new indexes for the assessment of autonomic balance in elite soccer players. Int J Sports Physiol Perform 10: 452–457. DOI: 10.1123/ijspp.2014-0235.

Poddar MG, Birajdar AC, Virmani J (2019). Automated classification of hypertension and Coronary artery disease patients by PNN, KNN, and SVM classifiers using HRV Analysis. Machine Learning in Bio-Signal Analysis and Diagnostic Imaging 99–125. DOI: 10.1016/B978-0-12-816086-2.00005-9.

Quintana M, Storck N, Lindblad LE, Lindvall K, Ericson M (1997). Heart rate variability as a means of assessing prognosis after acute myocardial infarction: A 3-year follow-up study. Eur Heart J 18: 789–797. DOI: 10.1093/oxfordjournals.eurheartj.a015344.

Rahman F, Pechnik S, Gross D, Sewell L, Goldstein DS (2011). Low frequency power of heart rate variability reflects baroreflex function, not cardiac sympathetic innervation. Clin Auton Res 21: 133–141. DOI: 10.1007/s10286-010-0098-y.

Rupprecht S, Finn S, Hoyer D, Guenther A, Witte OW, Schultze T, Schwab M (2020). Association between systemic inflammation, carotid arteriosclerosis, and autonomic dysfunction. Transl Stroke Res 11: 50–59. DOI: 10.1007/s12975-019-00706-x.

Sajadieh A, Nielsen OW, Rasmussen V, Hein HO, Hansen JF (2006). C-reactive protein, heart rate variability and prognosis in community subjects with no apparent heart disease. J Inter Med 260: 377–387. DOI: 10.1111/j.1365-2796.2006.01701.x.

Schlenker J, Nedělka T, Riedlbauchová L, Socha V, Hána K, Kutílek P (2014). Recurrence quantification analysis: a promising method for data evaluation in medicine. Eur J Biomed Inform 10: en35–en40. DOI: 10.24105/ejbi.2014.10.1.7.

Shaffer F, Ginsberg JP (2017). An overview of heart rate variability metrics and norms. Front Public Health 5: 46. DOI: 10.3389/fpubh.2017.00258.

Shah PK (2019). Inflammation, infection and atherosclerosis. Trends Cardiovasc Med 29: 468–472. DOI: 10.1016/j.tcm.2019.01.004.

Shahnawaz MB, Dawood H (2021). An Effective Deep Learning Model for Automated Detection of Myocardial Infarction Based on Ultrashort-Term Heart Rate Variability Analysis. Math Probl Eng, 13 p. DOI: 10.1155/2021/6455053.

Sharma M, Acharya UR (2019). A new method to identify coronary artery disease with ECG signals and time-Frequency concentrated antisymmetric biorthogonal wavelet filter bank. Pattern Recognit Lett 125: 235–240. DOI: 10.1016/j.patrec.2019.04.014.

Shi M, Zhan C, He H, Jin Y, Wu R, Sun Y, Shen B (2019). Renyi distribution entropy analysis of short-term heart rate variability signals and its application in coronary artery disease detection. Front Physiol 10: 809. DOI: 10.3389/fphys.2019.00809.

Shukla RS, Aggarwal Y (2018a). Nonlinear heart rate variability based artificial intelligence in lung cancer. J Appl Biomed 16: 145–155. DOI: 10.1016/j.jab.2017.12.002.

Shukla RS, Aggarwal Y (2018b). Time-domain heart rate variability-based computer-aided prognosis of lung cancer. Indian J Cancer 55: 61–65. DOI: 10.4103/ijc.IJC_395_17.

Singh R, Arbaz M, Rai NK, Joshi R (2019). Diagnostic accuracy of composite autonomic symptom scale 31 (COMPASS-31) in early detection of autonomic dysfunction in type 2 diabetes mellitus. Diabetes Metab Syndr Obes 12: 1735–1742. DOI: 10.2147%2FDMSO.S214085.

Singh RS, Gelmecha DJ, Sinha DK (2022). Expert system based detection and classification of coronary artery disease using ranking methods and nonlinear attributes. Multimed Tools Appl 81: 19723–19750. DOI: 10.1007/s11042-021-11528-1.

Sopic D, Aminifar A, Aminifar A, Atienza D (2018). Real-time event-driven classification technique for early detection and prevention of myocardial infarction on wearable systems. IEEE Trans Biomed Circuits Syst 12: 1–11. DOI: 10.1109/TBCAS.2018.2848477.

Stein PK, Kleiger RE (1999). Insights from the study of heart rate variability. Annu Rev Med 50: 249–261. DOI: 10.1146/annurev.med.50.1.249.

Sztajzel J (2004). Heart rate variability: a noninvasive electrocardiographic method to measure the autonomic nervous system. Swiss Med Wkly 134: 514–522.

Takakura IT, Hoshi RA, Santos MA, Pivateli FC, Nobrega JH, Guedes DL, et al. (2017). Recurrence plots: a new tool for quantification of cardiac autonomic nervous system recovery after transplant. Braz J Cardiovas Surg 32: 245–252. DOI: 10.21470/1678-9741-2016-0035.

Tan JH, Hagiwara Y, Pang W, Lim I, Oh SL, Adam M, et al. (2018). Application of stacked convolutional and long short-term memory network for accurate identification of CAD ECG signals. Comput Biol Med 94: 19–26. DOI: 10.1016/j.compbiomed.2017.12.023.

Tarvainen MP, Niskanen JP, Lipponen JA, Ranta-Aho PO, Karjalainen PA (2014). Kubios HRV – heart rate variability analysis software. Comput Methods Programs Biomed 113: 210–220. DOI: 10.1016/j.cmpb.2013.07.024.

Tristani FE, Kamper DG, McDermott DJ, Peters BJ, Smith JJ (1977). Alterations of postural and valsalva responses in coronary heart disease. Am J Physiol 233: H694–699. DOI: 10.1152/ajpheart.1977.233.6.H694.

Trivedi GY, Saboo B, Singh RB, Maheshwari A, Sharma K, Verma N (2019). Can decreased heart rate variability be a marker of autonomic dysfunction, metabolic syndrome and diabetes? J Diabetol 10: 48–56. DOI: 10.4103/jod.jod_17_18.

Verde L, De Pietro G (2019). A neural network approach to classify carotid disorders from Heart Rate Variability analysis. Comput Biol Med 109: 226–234. DOI: 10.1016/j.compbiomed.2019.04.036.

Xhyheri B, Manfrini O, Mazzolini M, Pizzi C, Bugiardini R (2012). Heart rate variability today. Prog Cardiovasc Dis 55: 321–331. DOI: 10.1016/j.pcad.2012.09.001.